Application of super-virtual seismic refraction interferometry to enhance first arrivals: A case study from Saudi Arabia

Abdulrahman Alshuhail, EXPEC Advanced Research Center, Saudi Aramco
Ali Aldawood and Sharif Hanafy, King Abdullah University of Science and Technology

Complex near-surface anomalies are one of the main onshore challenges facing seismic data processors. Refraction tomography is becoming a common technology to estimate an accurate near-surface velocity model. This process involves picking the first arrivals of refracted waves. One of the main challenges with refraction tomography is the low signal-to-noise ratio characterizing the first-break waveform arrivals, especially for the far-offset receivers. This is especially evident in data recorded using reflection acquisition geometry. This low signal-to-noise ratio is caused by signal attenuation due to geometrical spreading of the seismic wavefield, near-surface-generated noise, and amplitude absorption. Super-virtual refraction interferometry improves the quality of the first-break picks by enhancing the amplitude of the refracted waves and attenuating the amplitude of the random noise.

The theory of refraction interferometry was developed by Dong et al. (2006) and later Bharadwaj and Schuster (2010) successfully applied the technique. Dong et al. correlate a pair of traces to give $\phi(A|B)_x$, where A and B are the geophone positions and x is the source position. The resulting virtual trace has a virtual refraction arrival time of $\tau_{xB} - \tau_{xA}$. Repeating this procedure for any postcritical source position leads to a virtual trace of the same virtual refraction traveltime. Stacking the correlated traces over all postcritical source positions yields a trace with a virtual refraction event that has an enhanced signal-to-noise ratio. This enhancement can be as high as $\sqrt{N}$, where N is the number of sources that contribute to the generation of this particular virtual head wave. They demonstrate this method on land data shot over a salt dome in Utah and later Nichols et al. (2010) showed its effectiveness in a hydrogeophysical research site in Idaho.

A problem with refraction interferometry is that, if only the head wave arrivals are correlated with one another, the virtual head-wave trace has the correct moveout pattern. It has an unknown excitation time, so as a remedy, Dong et al. suggested that the source be "virtually" relocated to the surface by calibrating the virtual stacked refraction trace to an observed traveltime in the raw data. Another problem is that correlation of traces typically decreases the source-receiver offset of the virtual trace because traveltimes are subtracted and are associated with shorter raypaths. To overcome this, Bharadwaj and Schuster, Mallinson et al. (2011), and Hanafy et al. (2011) presented an extension of refraction interferometry so that the receiver spread could be extended to its maximum recording extent, and the absolute arrival time can be properly accounted for. This new method creates virtual far-offset refraction arrivals by

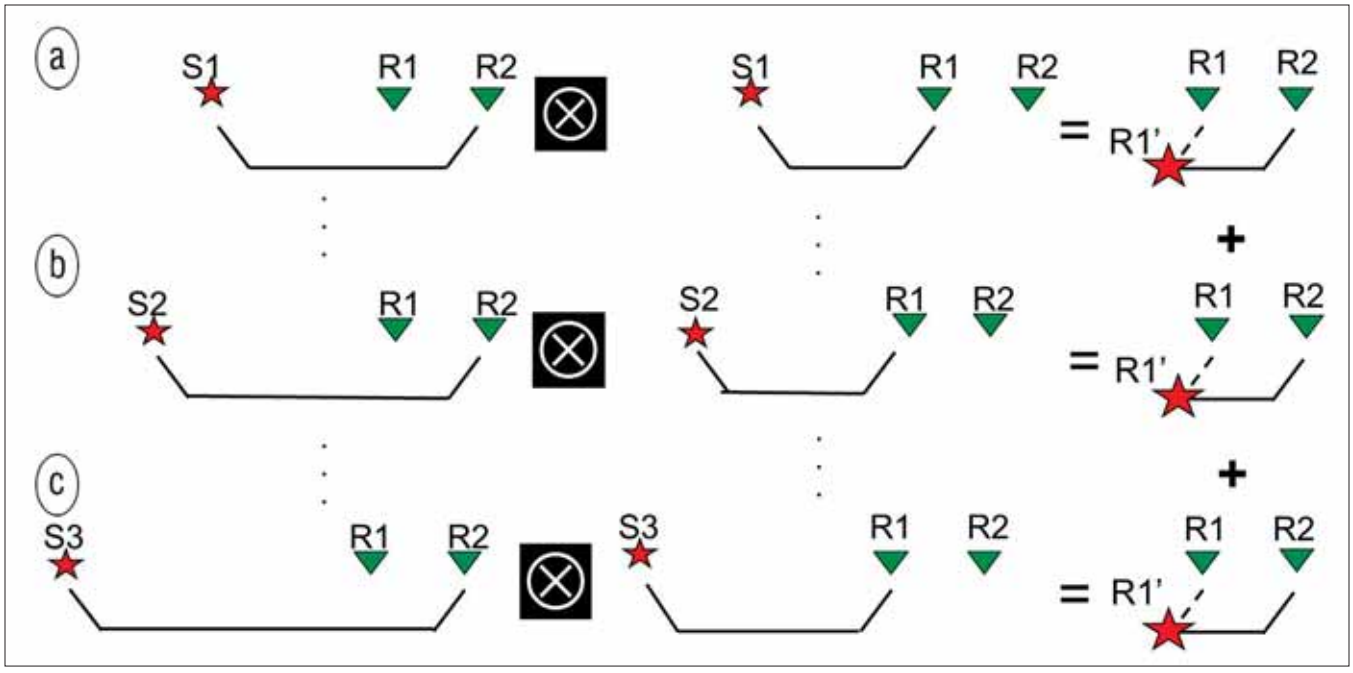

Figure 1. *(a) Cross-correlating the traces of refracted arrivals at* R1 *and* R2 *would redatum the source to the refractor at* R1′. *This virtual source will have a trace traveling from* R1′ *to* R2 *with a negative excitation time equal to the time between R1 and R1′. (b) Cross-correlating the traces using a different source position (*S2*) but with the same receiver pair (*R1 *and* R2*) generates the same virtual source trace as in (a). (c) As long as the receiver pair (R1 and* R2*) is present in a particular shot gather, then it is possible to obtain a trace that has the same raypath as in (a) for stacking.*

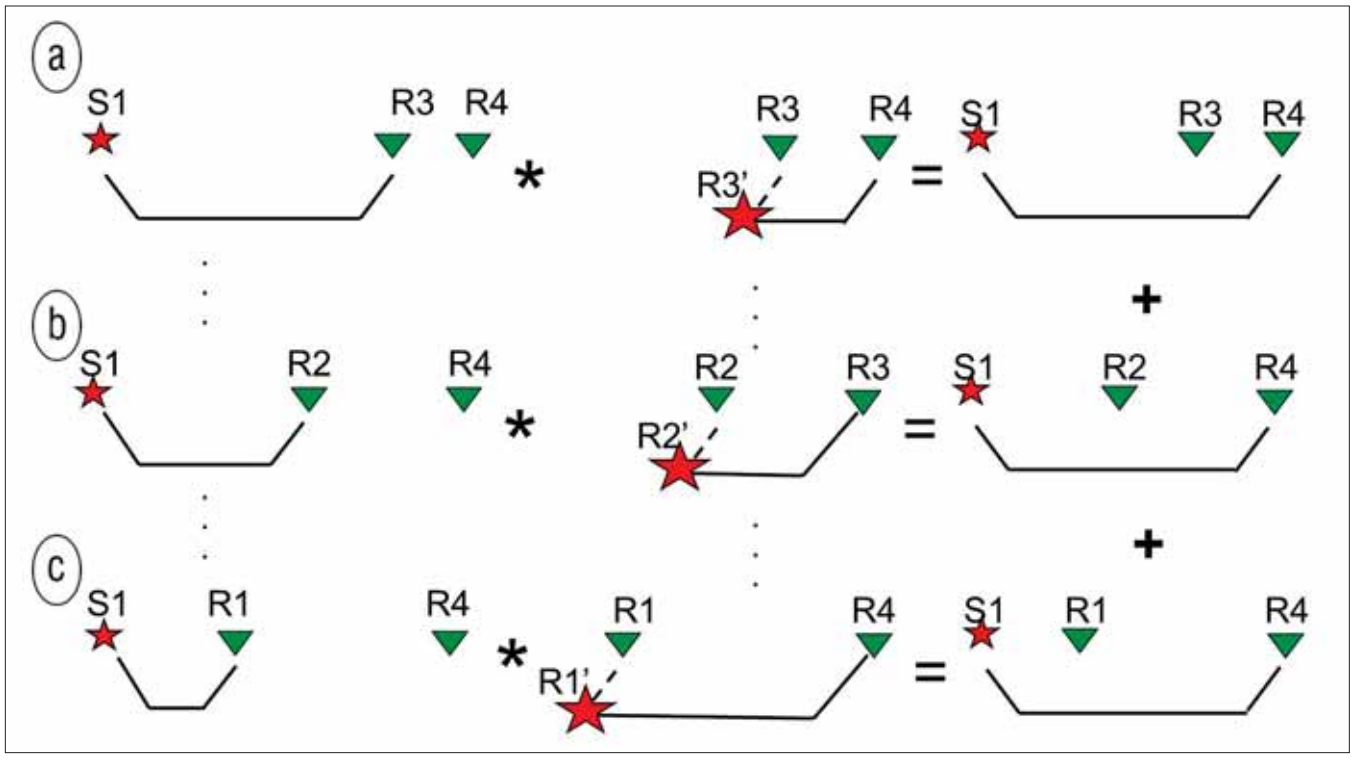

Figure 2. *(a) Convolving the traces of refracted arrival of the actual source to* R3 *and the virtual source at* R3′ *to* R4*, would redatum the source back to the surface (at* S1*). The receiver is located at* R4 *and the negative time component is removed due to adding the same time component but with positive sign. (b) Convolving the traces using traces of different virtual sources would generate the same trace as in (a). (c) It is possible to sum over all virtual traces that have a virtual source located between* S1 *and* R4*.*

a combination of both correlation and stack, and convolution and stack of traces with one another to create what is denoted as super-virtual refraction traces.

Theory

Let us assume a source at S and two receivers at R3 and R4 inside an arbitrary acoustic medium. The surface is surrounded by a closed surface. The reciprocity equation of correlation type for the far-field approximation in the frequency domain (Wapenaar and Fokkema, 2006) is given as:

$$Im[\mathrm{G}(\mathrm{R4}|\mathrm{R3}')^{virtual}] = k\int_{post\text{-}crit\ sources} G(R3|S)^{*}G(R4|S)dS \quad (1)$$

where i = $\sqrt{-1}$, k is the wavenumber of the head wave, and $G(R3|S)$ and $G(R4|S)$ are the recorded Green's functions from source S to receivers $R3$ and $R4$, respectively. The result of the cross-correlation $G(R4|R3')$virtual is a virtual source located at R3′ (the point where the raypaths to R3 and R4 diverge). The integration surface (So + S∞) reduces to So due to the Wapenaar anti-radiation condition which states that for a sufficiently heterogeneous medium which assumes little interactions at infinity, the recorded wavefield is negligible.

The excitation time of the virtual source is equal to the time it takes a seismic wave to travel between $R3$ and $R3'$ (Mallinson et al.). Figure 1a shows the result of cross-correlation where the dashed line indicates the negative time component. The virtual source is now independent of source position; thus the virtual source can be generated for different sources that have the same receiver pair. Figures 1b and 1c show that the same virtual source trace can be obtained using different shot positions with the same receiver pair. Hence the traces generated using the virtual sources are stacked to increase the signal-to-noise ratio.

The trace of the virtual source and an actual trace that travels to $R3$ are convolved to redatum the source back to the surface, remove the effect of negative time, and achieve a second stack. The reciprocity equation of convolution type in the far-field approximation gives the new redatum gather, $G(R4|S)^{super}$ according to the following expression:

$$\mathrm{G}(R4|S)^{super} = 2ik\int_{virtshot\ line} G(R3'|R4)^{virtual}\, G(R3|S)dR3 \quad (2)$$

where i = $\sqrt{-1}$, k is the wavenumber of the head wave, and $G(R3'|R4)^{virtual}$ is the stacked trace obtained by Equation 1. The superscript in the new redatumed Green's function $G(R4|S)^{super}$ is to indicate that this trace is different from the original recorded Green's function $G(R4|S)$, which is used in the reciprocity equation of correlation type (Equation 1). Figure 2a shows the redatuming process occurring in the convolution phase. Notice that, just as in the cross-correlation phase, the redatumed event in the convolution phase is now independent of virtual source position. Therefore it is possible to stack over the virtual source position. This is the second stack applied to the refracted data in order to achieve superior signal-to-noise ratio. Figures 2b and 2c depict that for different virtual source positions it is possible to obtain the same final trace. This new Green's function is a result of two redatuming steps and in-

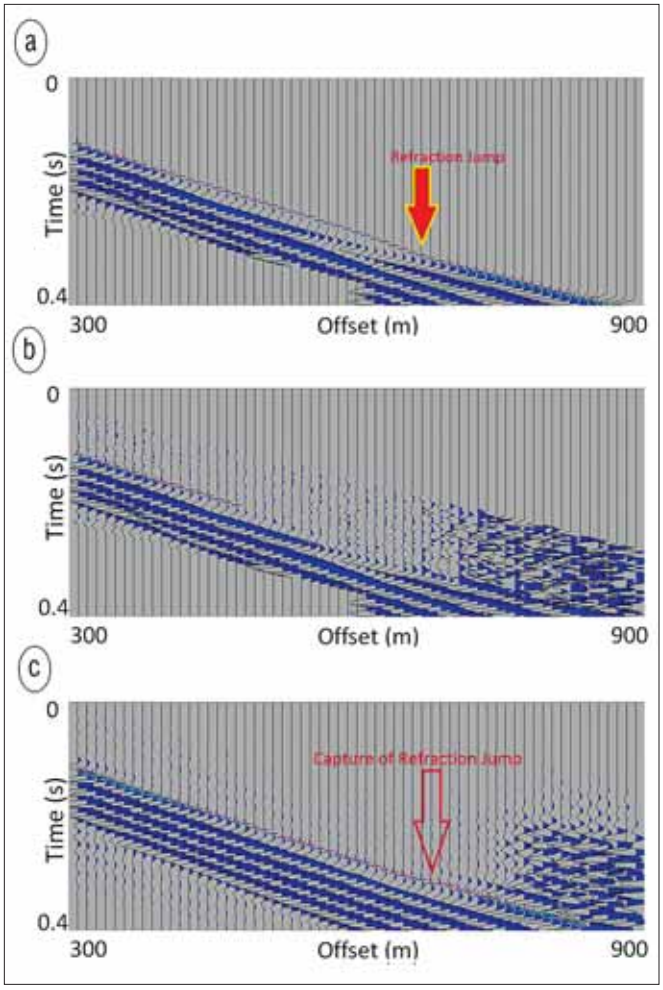

Figure 3. *(a) The synthetic data recorded before adding any noise; the first arrival is clear for picking. This will be used to validate the supervirtual picks. (b) Adding random noise masked the first arrival; hence the offset of the picks was limited. (c) The traces after applying super-virtual refraction interferometry; the random noise is now attenuated and the signal (refracted arrival) has been enhanced.*

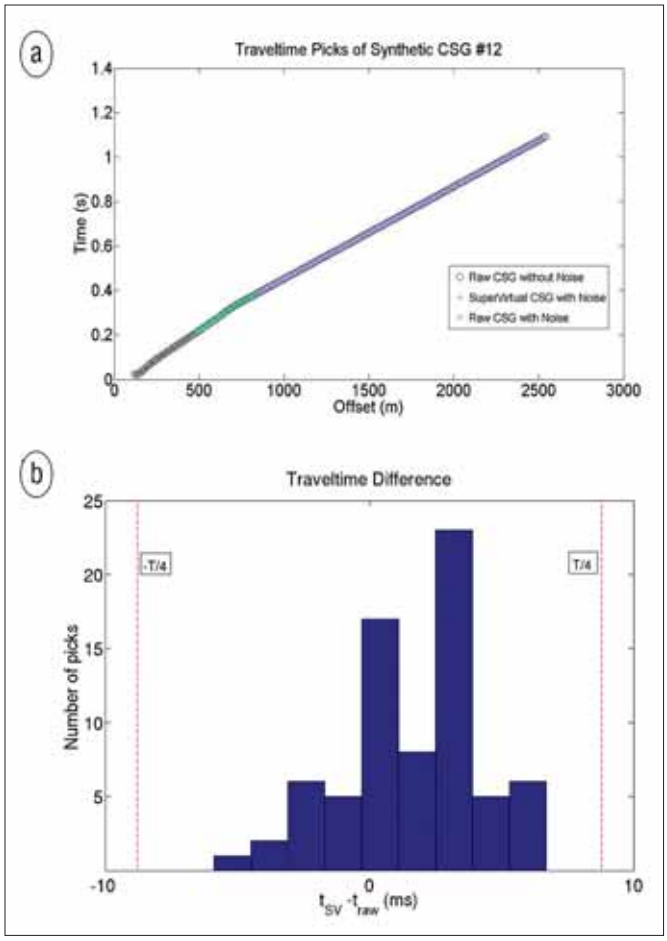

Figure 4. *(a) The traveltime picks are plotted versus offset. Note that after applying super-virtual refraction interferometry, the number of traveltime picks is almost doubled due to the increase in signal-to-noise ratio. (b) A histogram showing the difference between traveltime picks on super-virtual and noise-free synthetic data. Red lines indicate the* T/4 *limit.*

volves two stacking operations: one in the correlation phase and one in the convolution phase.

Synthetic data example

Prior to applying the super-virtual refraction interferometry theory on real data acquired using reflection geometry, the technique was tested on synthetic data with similar geometry to the real data. The synthetic data are generated using a finite-difference solution to the acoustic wave equation. Moreover, the number of sources generated was 23 with a source spacing of 10 m; each shot gather contained 243 receivers with 10-m interval spacing. Figure 3a shows the results obtained using a finite-difference modeling (note the green plus signs indicate the first picks). Notice that the refraction jumps are clearly visible. Refraction jumps refer to the crossover distance where a different refractor arrival becomes the first arrival.

Random noise was added to all the synthetic traces so that the refracted arrivals are no longer clearly visible. Figure 3b shows the same common-shot gather as in Figure 3a but with random noise added. It is difficult to follow the refracted first arrival and the refractor jump is no longer visible. This is because at this offset the noise level is becoming comparable to the signal level which is making the process of distinguishing between the signal and noise difficult. The mean value of signal-to-noise ratio of the common-shot gathers was calculated to be two.

Super-virtual refraction interferometry was applied to the synthetic data. This increased the signal-to-noise ratio dramatically due to the two stacking operations following each redatuming step. Therefore, the previously masked first-break refracted arrivals and the refraction jump were now clearly visible and easier to pick. Figure 3c shows the result of applying super-virtual refraction interferometry on the same traces as in Figures 3a and 3b.

One can compare the traveltime picks versus offset for all three data sets for one common-shot gather (in our case we chose CSG 12). In the noise-free synthetic data set, it was possible to pick all the first arrivals (up to 2430 m). After adding

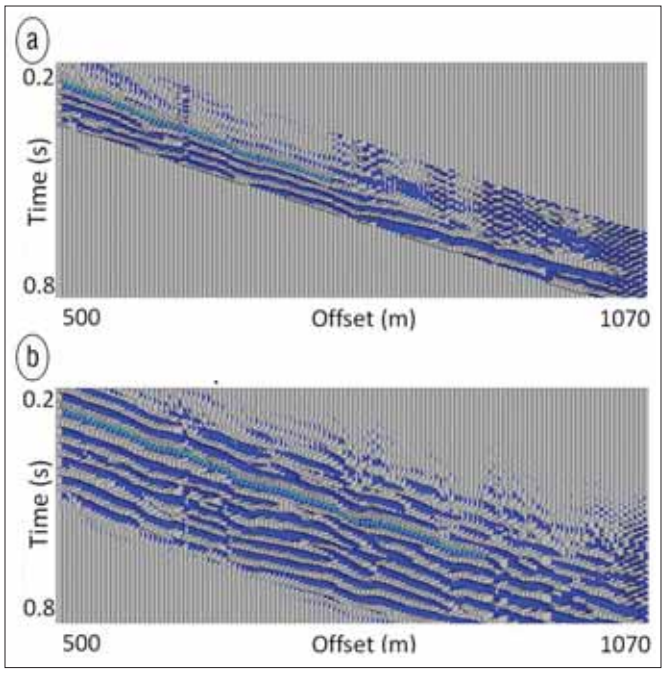

Figure 5. *(a) A windowed common-shot gather of the raw real data. The green plus signs indicate the first arrival picks. (b) The same windowed section after applying super-virtual refraction interferometry. The refracted arrival is enhanced and picking the first arrival could be done for farther offsets.*

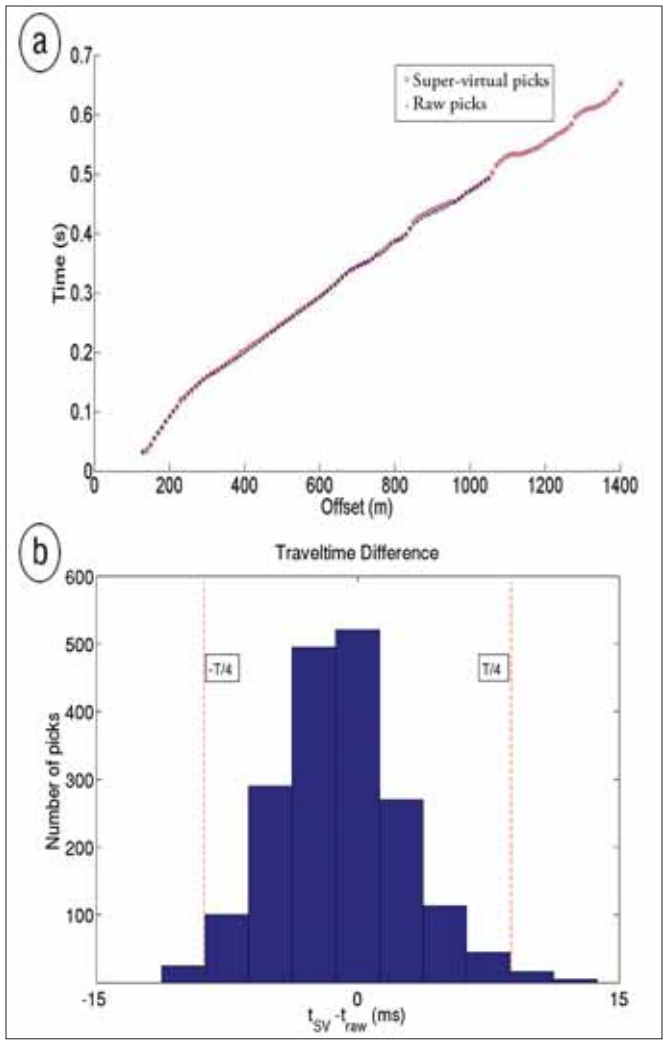

Figure 6. *(a) The picked traveltime for both the super-virtual and the raw data are displayed versus offset. Note that they coincide with the near offsets. (b) The difference between the first-arrival traveltime of the super-virtual and the raw picks. Note that the difference between the picks lies within a quarter of a cycle* (T/4).

noise, the first-break picking could be reliably performed up to an offset of about 480 m. After applying super-virtual refraction interferometry, picking could be done up to an offset of 910 m. Thus, super-virtual refraction interferometry was able to extend the first-break picking to a usable offset range by almost 90%. Figure 4a shows the traveltime picks versus offset for a common-shot gather for all three data sets. To ensure that the picking is done on the same event without any cycle skipping, the difference between the traveltime picks was calculated between the super-virtual and noise-free synthetic picks. All the picks fell within a quarter of a cycle (T/4). This could be considered as a quality assurance because the traveltime picks are almost identical to the picks obtained from a common-shot gather with pure signal. Figure 4b shows a histogram of the difference between the picks. Notice that almost all the events have a traveltime difference of less than a quarter of a cycle (red line indicates the quarter of the cycle).

Field data example

Super-virtual refraction interferometry has been tested on a land data set obtained in Saudi Arabia. The geometry is designed for reflected-wave acquisition. As in the synthetic example, the number of receivers is 243 with 10-m interval spacing; and the shot-interval spacing is 10 m. Due to irregularities in the source line position, only 23 common-shot gathers are chosen to apply the methodology.

A window is applied around the region of the first arrivals. The smaller the window, the less the artifacts appear after applying super-virtual refraction interferometry (Figure 5a). The first arrivals of the traces are clear up to 600-m offset; beyond this offset, the signal-to-noise ratio is very low. At approximately 750 m, it is difficult to distinguish the signal from the noise; thus picking the first arrival is not possible using conventional methods. Figure 5a illustrates a zoomed version of the common-shot gather.

Super-virtual refraction interferometry is applied to the windowed land data set. The signal-to-noise ratio of the refracted arrivals is now significantly increased and the random noise is attenuated. This enables picking the first arrival at farther offsets. Figure 5b shows the results after applying super-virtual refraction interferometry. To validate the accuracy of the picked traveltimes, first-arrival times are picked in the super-virtual gather and compared to the raw data picks (Figure 6a). The difference in the common traveltimes picks is mostly within a quarter of a period (Figure 6b).

The first-arrival picks are inverted to obtain a near-surface 2D velocity tomogram. The obtained tomograms show that

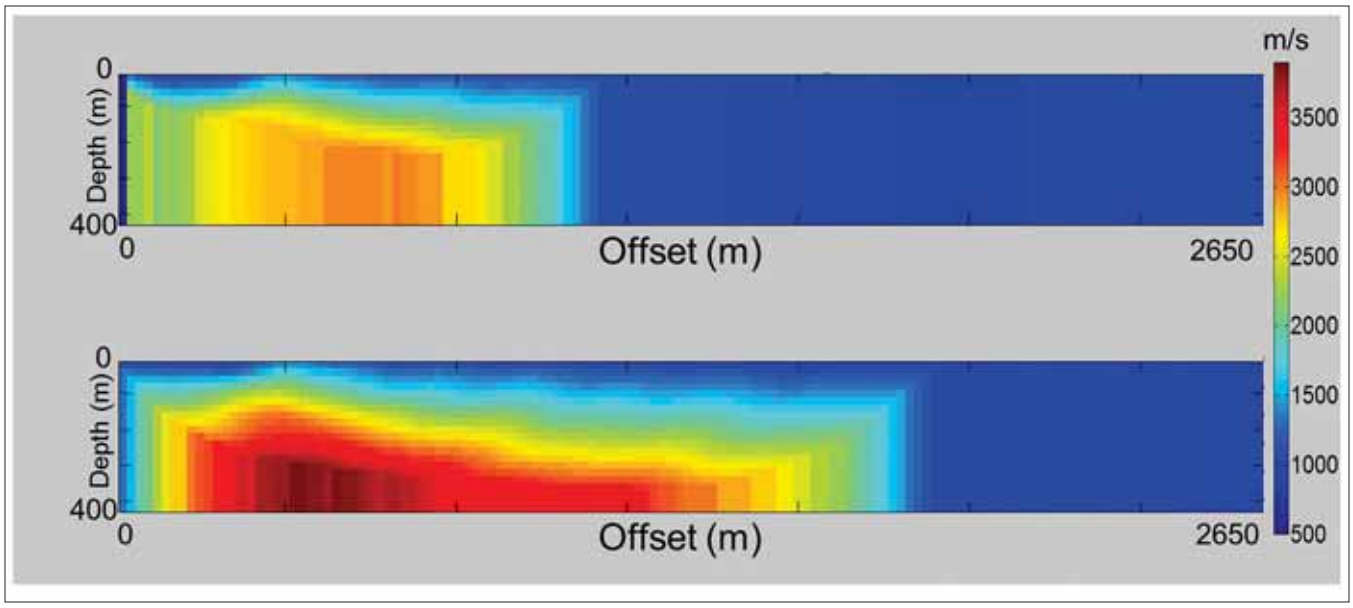

Figure 7. *(top) The inverted velocities using the raw first-arrival picks only. (bottom) The inverted velocities using the first-arrival picks after applying super-virtual refraction interferometry. Note that the aperture is doubled and the depth of investigation is deeper.*

the aperture has almost doubled and the reliability increased (due to an increased ray illumination). Also, because the events of interest are dipping, the depth of investigation has also increased after adding longer-offset traveltime picks. Generally, there are more features in the super-virtual section due to the extra picks (Figure 7). It should be noted that cross-correlation creates "ringier" super-virtual seismograms, which may be an additional complication but that can be addressed with an additional deconvolution step.

Wavelet distortion

When applying the cross-correlation and convolution processes, the seismic wavelet is no longer preserved. What is obtained is the result of cross-correlating and convolving two similar wavelets. This distorts the wavelet and creates side lobes that may confuse the first-break picker (Figure 8). One method to overcome this obstacle is to pick the first arrival for a couple of near-offset traces from the raw section (i.e., before applying super-virtual refraction interferometry). Then apply super-virtual refraction interferometry on the data set, and load the previous picks on top of the super-virtual section. Subsequently the refracted arrival will be identified and picking can resume to longer offsets. Another method to overcome this effect is to add an additional deconvolution step.

Extending from 2D to 3D

Extending super-virtual refraction interferometry from 2D to 3D is a great challenge. The problem is that current 3D acquisition surveys have few sources that generate common-refractor raypaths between the receivers due to the sparseness of source-receiver field configuration. Alternatively, in a dense 3D survey, there is a higher probability of common refractor overlap and thus super-virtual refraction interferometry is expected to enhance the first breaks as well.

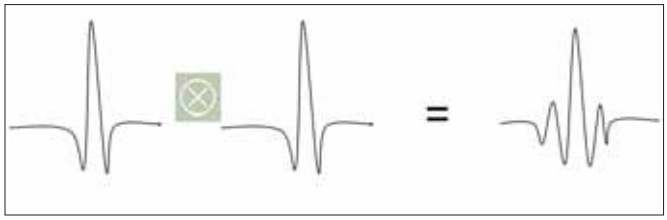

Figure 8. *The result of cross-correlating similar wavelets. Notice the generated side lobes that may influence the first-break picking.*

Conclusion

Using the super-virtual refraction interferometry method, the signal-to-noise ratio of far-offset refracted wave arrivals is expected to increase by approximately a factor of $\sqrt{N}$ where N is the number of actual sources and virtual sources used in the intereformetric summation. Super-virtual refracted arrivals are generated in two steps; the first step involves the cross-correlation and stacking of the data to generate traces with virtual head-wave arrivals and the second step entails the convolution and stacking of the data with the virtual traces to enhance head-wave arrivals.

Super-virtual refraction interferometry has been applied to a data set with a complex near surface from Saudi Arabia. Although the acquisition geometry employed is optimized for seismic reflection acquisition, the method has proven useful to extract and enhance the refracted arrivals in the data set. The resulting tomograms show that the aperture and depth of investigation have increased, producing more reliable near-surface models. TLE

References

Bharadwaj, P. and G. T. Schuster, 2010, Extending the aperture and increasing the signal-to-noise ratio of refraction surveys with super-virtual interferometry: AGU Annual Meeting Abstracts.

Dong, S., J. Sheng, and G. T. Schuster, 2006, Theory and practice of refraction interferometry: 76th Annual Meeting, SEG, Expanded Abstracts, 3021–3025.

Hanafy, S., O. AlHagan, and F. Al-Tawash, 2011, Super–virtual refraction interferometry: Field data example over a colluvial wedge: 81st Annual Meeting, SEG, Expanded Abstracts, 3814–3818.

Mallinson, I., P. Bharadwaj, G. T. Schuster, and H. Jakubowicz, 2011, Enhanced refractor imaging by supervirtual interferometry: The Leading Edge, **30**, no. 5, 546–550, doi:10.1190/1.3589113.

Nichols, J., D. Mikesell, and K. V. Wijk, 2010, Application of the virtual refraction to near-surface characterization at the boise hydrogeophysical research site: Geophysical Prospecting, **58**, 1011–1022.

Wapenaar, K. and J. Fokkema, 2006, Green's function representations for seismic interferometry: Geophysics, **71**, no. 4, SI33–SI46, doi:10.1190/1.2213955.

Acknowledgments: We thank Saudi Aramco for the opportunity to work on this project and publish the results; in particular we thank Panos Kelamis and Tim Keho for their support of this project. We are grateful to Andrey Bakulin, Constantine Tsingas, and Emad Hemyari (all from Saudi Aramco) for their valuable comments and suggestions, which improved the quality of this article. We are thankful to Gerard Schuster (KAUST) for introducing us to this technology and helping us throughout the project.

Corresponding author: abdulrahman.shuhail@aramco.com